Transp Porous Med (2011) 89:97–120
DOI 10.1007/s11242-011-9754-5

Study of Microscopic and Macroscopic Displacement Behaviors of Polymer Solution in Water-Wet and Oil-Wet Media

Hamid Emami Meybodi · Riyaz Kharrat ·
Xiaoqi Wang

Received: 22 August 2008 / Accepted: 5 March 2011 / Published online: 24 March 2011
© Springer Science+Business Media B.V. 2011

Abstract Performance of a polymer flood process requires the knowledge of rheological behavior of the polymer solution and reservoir properties such as rock wettability. To provide a better understanding of effects of polymer chemistry and wettability on the performance of a polymer flood process, a comprehensive experimental study was conducted using a two-dimensional glass micromodel. A series of water and polymer flood processes were carried out at different polymer molecular weights, degrees of polymer hydrolysis, and polymer concentrations in both water-wet and oil-wet systems. Image processing technique was applied to analyze and compare microscopic and macroscopic displacement behaviors of polymer solution in each experiment. From micro-scale observations, the configuration of connate water film, polymer solution trapping, flow of continuous and discontinuous strings of polymer solution, piston-type displacement of oil, snap-off of polymer solution, distorted flow of polymer solution, emulsion formation, and microscopic pore-to-pore sweep of oil phase were observed and analyzed in the strongly oil-wet and water-wet media. Rheological experiments showed that a higher polymer molecular weight, degree of hydrolysis, and concentration result in a higher apparent viscosity for polymer solution and lower oil–polymer viscosity ratio. It is also shown that these parameters have different impacts on the oil recovery in different wettabilities. Moreover, a water-wet medium generally had higher recovery in contrast with an oil-wet medium. This experimental study illustrates the successful application of glass micromodel techniques for studying enhanced oil recovery (EOR) processes in five-spot pattern and provides a useful reference for understanding the displacement behaviors in a typical polymer flood process.

H. Emami Meybodi (✉)
Department of Chemical and Petroleum Engineering, University of Calgary, Calgary, AB, Canada
e-mail: hemamime@ucalgary.ca

H. Emami Meybodi · R. Kharrat
Tehran Faculty of Petroleum Engineering, Petroleum University of Technology, Tehran, Iran

X. Wang
Petroleum Technology Research Center, University of Regina, Regina, SK, Canada

Keywords Polymer flooding · Wettability · Glass micromodel · Microscopic and macroscopic displacement · Oil recovery

List of Symbols

BT	Breakthrough time
C_p	Polymer concentration
EOR	Enhanced oil recovery
k	Absolute permeability (Darcy)
$\mathrm{MW_p}$	Polymer molecular weight (g/mol)
OOIP	Original oil in place, dimensionless
PHPA	Partially hydrolyzed polyacrylamide
PV	Pore volume (cm^3)
R_B	Breakthrough recovery
$R_{1.5\,\mathrm{IPV}}$	Recovery at 1.5 injected pore volume

1 Introduction

Since early 1900s, waterflooding has been used to maintain the reservoir pressure and also to sweep out oil from a reservoir (Uren and Fahmy 1927). However, due to unfavorable water–oil mobility ratio of medium-heavy oil reservoirs and the heterogeneity of some reservoirs, this process has sometimes been substituted by polymer flooding. Pye (1964) and Sandiford (1964) established the fact that mobility of a brine used in waterflooding could be greatly reduced by addition of small amounts of water-soluble polymer (i.e., hydrolyzed polyacrylamide), which may consequently lead to a higher oil recovery (Chang 1978; Gogarty 1967; Green and Willhite 2003; Jewett and Schurz 1970; Needham and Doe 1987; White et al. 1973). Generally, in oil industry, polymers have been used for two main purposes: conformance control (i.e., gelled-polymer treatment) and mobility control (i.e., polymer flooding), which the later is the focus of this article.

During a typical polymer flooding process, a water-soluble polymer with a very high molecular weight is added into the brine to increase the viscosity and improve the sweep efficiency of oil by controlling the mobility ratio, which is ratio of the polymer solution mobility to the oil mobility. The mobility of a polymer solution is defined as the ratio of its relative permeability to its apparent viscosity (Donaldson et al. 1989).

Polymer flooding success hinges not only on the maintaining of mobility control but also effectiveness of the chemicals. Numerous studies have shown that polymer retention is the main reason for permeability reduction in porous media during a polymer flood process (Mungan 1969; Smith 1970; Sparlin 1975; Szabo 1975). Another important reason for permeability reduction caused by polymer solutions is the entrapment, which mostly occurs through low permeability zones (Mungan et al. 1966; Szabo 1975). Polymer can adsorb onto the grain surfaces of the most reservoirs. Basically, polymer coats the rock surfaces with a hydrophilic film. When water passes over the coat, it swells and reduces the effective permeability. In contrast, the swelling does not occur in the presence of oil. Therefore, the polymer solution can reduce its mobility to a large extent in low oil saturation zones and result in a high oil recovery (Sparlin 1975). Nonetheless, if the polymer slug is adsorbed or dispersed then the mobility ratio at the front may revert back to the water–oil mobility ratio.

In general, polymer solution increases the oil recovery by decreasing the water–oil mobility ratio, diverting the injected water from zones that have been swept, or through the effects of polymers on fractional flow (Needham and Doe 1987).

In the most field applications, polymer is combined with surfactants and alkalis to increase the sweep efficiency of different recovery methods (e.g., ASP, AP, and SP). Surfactants and alkalis influence the adsorption of the polymer onto the grain surfaces resulting in both detrimental and beneficial effects on the flow performance of the chemicals (Nasr-El-Din and Taylor 1993; Nilsson et al. 1997; Taugbol et al. 1995).

Prediction and evaluation of the performance of a polymer flood process, in a field project, requires the deep understanding of the rheological behavior of the polymer solution, reservoir heterogeneities (Emami Meybodi et al. 2008), and reservoir wettability. As one of the factors, reservoir wettability strongly affects the fractional flow and displacement efficiency of a polymer flood process. Therefore, it is necessary to study the physical relationship between fluids (i.e., brine and oil) and porous media.

The wettability (i.e., relative hydrophobic/hydrophilic nature of the mineral phases/ reservoir) plays an important role in determining the recovery factor. The reservoir wettability and its effects on oil recovery have been investigated extensively since 1950s (Anderson 1986, 1987). Before the 1950s oil reservoirs had been thought to be water-wet. Later, it was discovered that oil reservoirs could have wide range of wettabilities, i.e., water-wet, intermediate-wet, and oil-wet. However, most oil reservoirs have a non-uniform wettability called mixed-wet (Treiber et al. 1972). Basically, the original wettability of most reservoir rocks can be altered by the adsorption of polar compounds and/or the deposition of organic matter that was originally in the resident fluids such as crude oil (Anderson 1986). At the end of 1980s and the beginning of 1990s, numerous experimental studies were reported regarding the role of wettability in various aspects of oil recovery in waterflooding (Buckley and Morrow 1990; Cuiec and Anderson 1990; Dubey and Waxman 1991; Jadhunandan and Morrow 1995; Jia et al. 1991; Morrow 1990). Ideally, during a waterflood of an oil-wet system, the water-relative permeability increases and the oil relative permeability decreases. Then, the water will flow more easily in comparison with the oil, causing progressively earlier breakthrough and consequently higher residual oil saturation in the reservoir, i.e, the lower oil recovery (Anderson 1987). In contrast, waterflooding in a water-wet system is more efficient and the oil recovery is higher.

Broseta et al. (1995) have conducted a series of polymer flood experiments in glass micromodels under various wettabilities and saturation conditions with the purpose of characterizing polymer adsorption on hydrophobic surfaces and understanding the effects of residual oil upon polymer adsorption during polymer EOR process. They showed that the presence of residual oil reduces the polymer adsorption/retention in oil-wet porous media, whereas the inverse trend was observed in water-wet porous media. Elmkies et al. (2001) performed some core flood experiments to investigate the effect of wettability on polymer adsorption and oil/water relative permabilities. Their results indicated that polymer (i.e., polyacrylamide) adsorbs on the rock surface no matter what kind of wetting condition it is. However, the adsorption of hydrophilic polymer in partially oil-wet cores seems to indicate that the polymer restores part of the initial rock water wettability. In another core flood research, Dong et al. (2006) proposed that the influence of wettability on oil recovery of polymer flooding is minor for water-wet, oil-wet and neutral-wet Berea sandstones. Recently, Yadali Jamaloei and Kharrat (2009, 2010) investigated the wettability and morphology effects of porous media on microscopic and macroscopic behavior of polymer assisted dilute surfactant flooding using glass micromodel. Their results showed that the wettability and pore geometric properties in a porous medium greatly affect the instability of displacement front (e.g., viscous fingering) and the displacement mechanisms of microscopic two-phase flow (e.g., snap-off). In the most recent research, Romero-Zerón et al. (2010) applied MRI technique to visualize the performance of polymer flooding and to quantify the in-situ fluid saturation distribution in rocks with different wettabilities and they showed that polymer flooding is much more efficient in the strongly water-wet condition than preferentially oil-wet condition.

In this article, effect of wettability in polymer flooding has been examined by using a two-dimensional glass micromodel (one-quarter five-spot). Polymer solutions with different polymer-molecular weight, concentration, and degree of hydrolysis were injected into the micromodel at strongly oil-wet and water-wet conditions, respectively. Effect of these parameters, on oil recovery and configuration of displacement front was evaluated in two wetting conditions. In addition, the effect of medium wettability on microscopic displacement behaviors of polymer flooding was considered.

Glass micromodel was used in this work since the effect of wettability on microscopic mechanisms as well as macroscopic behavior (i.e., oil recovery value and configuration of displacement front) of the polymer flooding was required to be studied. The micromodel is a transparent artificial model of porous medium that can be used to simulate transport processes at the pore scale and also a powerful tool to efficiently restore different wettability states for a porous medium. According to the literature (Dawe and Zhang 1994; Haghighi and Yortsos 1997; Larsen et al. 2000; Waldraw 1980) most of the micromodel studies have been focused on qualitative investigations of phase displacements behavior, and only a few works used micromodels for both qualitative observations and quantitative measurements.

2 Experimental Set-Up, Materials, and Procedures

2.1 Experimental Set-Up

The micromodel set-up composed of four sections including cleaning system, fluid injection section, optical system, and micromodel holder. Figure 1 presents schematic diagram of the experimental set-up.

Cleaning was accomplished by flushing solvent through the micromodel using a pump, named Eldex pump. The Eldex pump pumps cleaning fluids (i.e., distilled water, methylene chloride, acetone, and toluene) from their containers into the micromodel. A precise pressure transducer and a high-accuracy low-flowrate pump, named Quizix pump, were used to control the flowrate of fluids through micromodel. The Quizix pump was able to inject at rates varying from 10^{-5} to $10\,\text{cm}^3\,\text{min}^{-1}$.

In this study, the majority of data acquisition was achieved through visual observation. Thus, it is important to use high-resolution optical equipment for image capturing and analysis. A computer-controlled linear drive system was used that allowed a magnifying video camera to be positioned automatically at any part of a micromodel and sequentially or continuously record the phases displacement occurring within the micromodel. The camera is capable of working at a magnification up to 200 times. While conducting an experiment, in addition to continuous video recording, pictures of the micromodel were digitally grabbed by a computer interface and recorded. These pictures are later used for image analysis and saturation measurement purposes. To analyze the results of the immiscible displacement experiments, it is necessary to measure the fluids' saturation variations within the micromodel. Sigma Scan® Pro 5.0 image analysis software and statistical analyses were used to obtain detailed characterization of the porous medium and also measurement of the fluid saturations from the micromodel microphotographs.

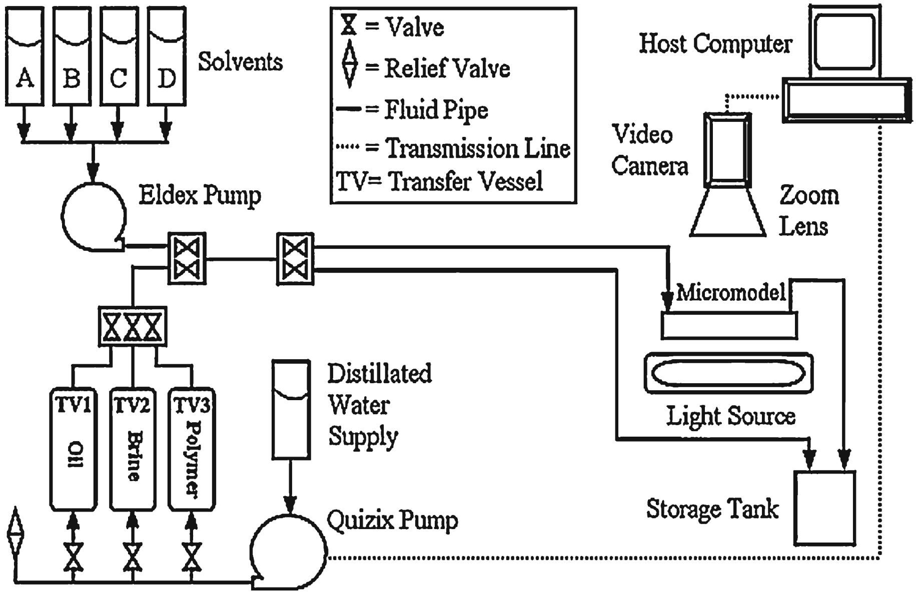

Fig. 1 Schematic of experimental apparatus (Emami Meybodi et al. 2008)

In order to generate the glass micromodels, first a pattern of a porous medium should be designed on a paper and then etched on a glass to create a synthetic porous structure whose aggregates represent an ideal porous medium. For this study, a two-dimensional pore network with a length of 60 mm and width of 60 mm was designed by Corel Draw® software. Triangular pore bodies were selected with the coordination number of 3. Aspect ratio of the pore network (i.e., ratio of pore body diameter to pore neck diameter) was 2.33. Figure 2 shows the homogenous designed pattern. The pattern was then etched onto the surface of a glass plate by using hydrofluoric acid. A second, optically flat, glass plate was then placed over the first, covering the etched pattern and thus creating an enclosed pore space. The cover plate had an inlet hole and an outlet hole drilled at either end, allowing fluids to be displaced through the network of pores. This combination was placed into a special oven (Blue M Standard Ultra-Temp® High-Temperature) that the temperature and heat flux are controlled automatically. The heating process started from ambient temperature to 724°C gradually, after this the oven cooled down slowly. This heating process known as fusing process was performed in order to make completely sealed micromodels.

When the micromodel was produced, some of the pattern properties were estimated by the software (e.g., porosity), but others could not be estimated by the pattern creation software (e.g., the absolute permeability and etched depth).

The soaking time of the micromodel glass in the hydrofluoric acid determined the depth of etching. Thus we could generate different micro-patterns with various etched depth. The depth of the etched area was measured by using Mitutoyo (NO3109F), which was an apparatus for measuring a micro depth. The apparatus consisted of a spindle, a thumb that could be levered to rise and lower, and a dial depth gauge that measured depths with a resolution of 0.001 mm and an accuracy of 0.001 mm. To measure the etched depth, first, the gauge was calibrated by placing the spindle head on a flat part of the glass, i.e., surface of glass that was considered as grains, and set zero. Then by placing the spindle head in the nearest pore

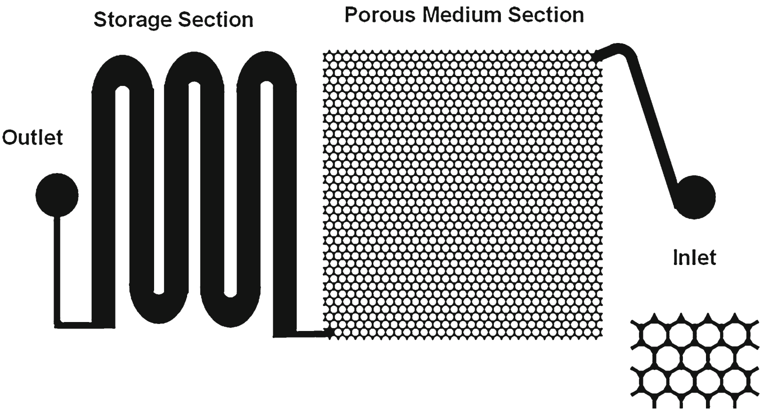

Fig. 2 Schematic of the two-dimensional micromodel pattern (Emami Meybodi et al. 2008)

body/neck, etched depth was shown on the gauge. This procedure was repeated on different pore bodies and necks to get an average etched depth. The average etched depth of the micromodel using in this study was uniform and equal to 0.045 mm.

The porosity of the micromodel was estimated to be $28.6 \pm 0.05\%$ using a combination of image analysis and the average etched depth as determined in the last paragraph. The image analysis was used to estimate the areal porosity of the model when it was filled with colored water.

Absolute permeability of the micromodel was measured by conducting one-dimensional flow experiments and using Darcy's law by recording pressure drops at numerous different flowrates. To determine the absolute permeability, which requires the condition of one-dimensional Darcy flow to be established, an one-dimensional micromodel with length of 60 mm and width of 10 mm was generated. The one-dimensional micromodel has the same structure, pore network, and average etching depth of the two-dimensional micromodel. The measured absolute permeability for the one-dimensional micromodel is 1.33 ± 0.09 Darcy. Based on the similarity of physical properties, it was assumed that absolute permeability of the two-dimensional micromodel is the same as the calculated permeability from one-dimensional micromodel. Further information about permeability measurement was presented elsewhere (Yadali Jamaloei and Kharrat 2009). Each determination test was repeated to examine the repeatability of the results.

2.2 Materials

West Paydar crude oil, with an API of 19.8^o measured at 26.5°C, was used as the oil sample. West Paydar is one of the oil fields located in Western Iran. The density and viscosity of crude oil at different conditions were measured using a digital densitometer (512P, Anton Paar®) and a rolling-ball viscometer (P/N, Chandler Engineering), respectively. Some of the crude oil physical properties are given in Table 1. It is worthwhile to note that, before saturating the micromodel with crude oil, the oil sample was filtered to remove any solid particle but not asphaltenes. Considering the very short duration of each experiment, it was expected that the asphaltenes and heavy components have minor effects on wettability alteration of water-wet medium.

Table 1 Crude oil properties at different temperatures

Temperature (°C)	15.5	21	26.5
Oil Density (kg/m^3)	933.2	929.9	926.2
Oil Viscosity (mPa.s)	142.0	101.8	74.9

Table 2 Properties of the polyacrylamides

Characteristics	Polymer 1	Polymer 2	Polymer 3
Molecular weight (g/mol)	1.6×10^6	8×10^6	12×10^6
Degree of hydrolysis (%)	25–30	20–25	20–25
Activity (%)	100	100	100

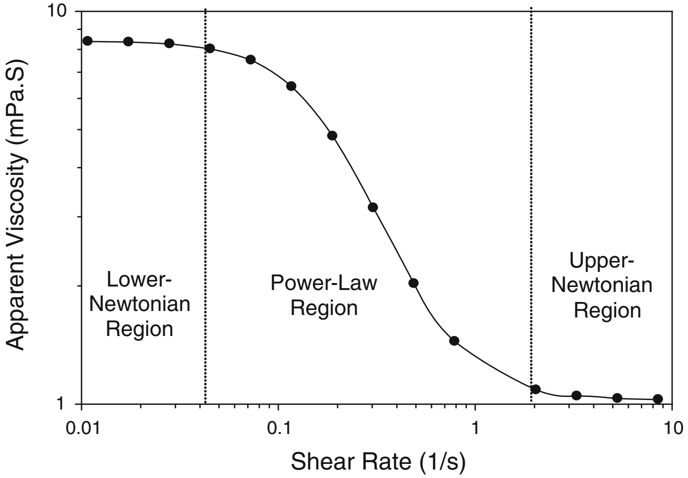

Fig. 3 Viscosity of the polymer solution versus shear rate

A synthetic brine with the concentration of 20,000 ppm was prepared by dissolving NaCl, $MgCl_2$, $CaCl_2$, and Na_2SO_4 (supplied by Merck, Germany, with the purities of 99.5, 98, 99.9, and 99.0%, respectively) into the distilled water. Concentrations of NaCl, $MgCl_2$, $CaCl_2$, and Na_2SO_4 in the synthetic brine were 1.7, 0.1, 0.3, and 0.01, respectively. These salt concentrations have been chosen according to the criteria mentioned by Romero-Zerón (2004). The salinity of connate water and polymer solution were selected as the same (i.e., 20,000 ppm) to avoid possible incompatibility between connate water and injected polymer solution.

Three partially hydrolyzed polyacrylamide polymers with different molecular weights were supplied by Research Institute of Petroleum Industry (RIPI), Iran, and used in experiments. Properties of these polymers are given in Table 2.

The rheologies of the polymer solutions were determined at low and high shear rates at 26°C. The determination of polymer solutions rheologies were carried out using a Physica MCR 300 rheometer (Anton Paar®). Rheology of one of the polymer solutions ($MW_p = 12 \times 10^6$ g/mol, 500 ppm) is shown in Fig. 3. In this figure, different rheologies for the polymer solution at different shear rates can be observed. According to the homogeneity of the micromodel and injection flowrate, low shear rate flow was expected during polymer floods. Therefore, the viscosity of polymer solution at the lower Newtonian region was considered in order to calculate the oil–polymer viscosity ratio. For instant, the oil–polymer viscosity ratio of the discussed polymer solution is 8.8. Rheological experiments showed that apparent viscosity increased with the molecular weight of polymer. Also, a higher degree of hydrolysis exhibited a greater apparent viscosity. In addition, an increase in polymer concentration increased the apparent viscosity of the solution, which was a mass effect as more polymer molecules were dissolved.

2.3 Experimental Procedures

To observe the effect of wettability in water and polymer flooding with different polymer molecular weights and concentrations in a synthetic porous medium, a homogenous micromodel was used. Two sets of experiment were performed to observe the performance of water and polymer flooding in water-wet and oil-wet media. In each set, the effects of polyacrylamide molecular weight and concentration were considered. Data related to the two sets of experiment are given in Table 3.

Before each experiment, the micromodel was cleaned with toluene (supplied by Merck, Germany with purity of 99.9%), methylene chloride (supplied by Merck, Germany), acetone (supplied by Merck, Germany with purity of 99.8%), and distilled water. After cleaning, the micromodel was vacuumed by a vacuum pump and saturated with the synthetic brine and then flooded with the crude oil to reach the connate water saturation. Then, water or polymer solution was injected from inlet port into the micromodel. In order to vacuum the micromodel and remove air bubbles and any fluid, the production port (outlet) was connected to the vacuum

Table 3 Data related to the all experiments

Test no.	Wetting nature	Fluid type	MW_p ($\times 10^6$ g/mol)	C_p (ppm)
1	Water-wet	Brine	–	–
2	Water-wet	PHPA	1.6	100
3	Water-wet	PHPA	1.6	300
4	Water-wet	PHPA	1.6	500
5	Water-wet	PHPA	8	100
6	Water-wet	PHPA	8	300
7	Water-wet	PHPA	8	500
8	Water-wet	PHPA	8	700
9	Water-wet	PHPA	12	100
10	Water-wet	PHPA	12	300
11	Water-wet	PHPA	12	500
12	Oil-wet	Brine	–	–
13	Oil-wet	PHPA	1.6	100
14	Oil-wet	PHPA	1.6	300
15	Oil-wet	PHPA	1.6	500
16	Oil-wet	PHPA	8	100
17	Oil-wet	PHPA	8	300
18	Oil-wet	PHPA	8	500
19	Oil-wet	PHPA	8	700
20	Oil-wet	PHPA	12	100
21	Oil-wet	PHPA	12	300
22	Oil-wet	PHPA	12	500

pump while the injection port (inlet) was plugged. Injection flowrate of 0.0006 $cm^3 min^{-1}$ (i.e., 1.2 ft/day) was chosen and held constantly in all performed experiments. All experiments were carried-out in ambient temperature of 26.0 ± 0.5°C.

The procedure to maintain the initial water-wet state of the micromodel is the modified procedure used by Romero-Zerón (2004), which is summarized as follows: (1) Rinsing micromodel with toluene to eliminate any residual oil, using the vacuum system, and removing the excess of liquids from micromodel; (2) Rinsing micromodel with acetone and removing excess of fluids; (3) Rinsing micromodel with distilled water and removing the excess of water; (4) Soaking micromodel with hydrochloric acid solution (20 v/v%) for several hours, and removing excess of acid from micromodel thoroughly after the soaking period, then rinsing micromodel with distilled water and removing excess of water; (5) Rinsing micromodel with acetone and removing excess of acetone; (6) Placing micromodel in oven and drying at 100°C for 1 h.

The procedure to alter the wettability of the micromodel to strongly oil-wet is as follows (Romero-Zerón 2004): (1) Rinsing micromodel thoroughly with sodium hydroxide for 1 h; (2) Rinsing micromodel thoroughly with distilled water to remove all residues, and then dry it in an oven at 200°C for at least 15 min; (3) Preparing a dilute solution of 2% tri chloro methyl silane (TCMS) and 98% dehydrate toluene (this solution should be prepared fresh daily); (4) Saturating the micromodel with the dilute solution for at least 5 min. A thin film immediately coats the micromodel's internal surface making it water repellent; (5) Rinsing the micromodel with methanol to remove excess siliconizing fluid; (6) Drying the micromodel in an oven at 100°C for 1 h to cure the silicone coating.

3 Results and Discussion

Some of the experiments were repeated to examine the reproducibility of the results, which include both qualitative observations and quantitative evaluations. For quantitative results, the values of oil recovery were changed only by average three percent, but trends have been remained unchanged. For observed qualitative evidences, although the frequency of occurrence of each phenomenon was slightly changed, the overall pictures describing the microscopic fluid flow mechanisms and macroscopic behavior of the process did not change. To be brief, the repeatability of the results was acceptable. Effects of wettability on waterflooding and polymer flooding that investigated qualitatively and quantitatively are explained in the following sections.

3.1 Microscopic Observations

To analyze the microscopic observations and microscale mechanisms at pore level, microshots captured by the digital microscope in tests 1 (water-wet, waterflood), 11 (water-wet, polymer flood), 12 (oil-wet, waterflood), and 22 (oil-wet, polymer flood) have been used. In the tests 11 and 22 all of the parameters affecting the polymer flooding performance remain unchanged and only the wettability of the porous medium is changed.

In a strongly oil-wet porous medium, initially there was no thick connate water film present on pore walls (grain surfaces). This is shown in Fig. 4a. In this figure, oil wetted the whole pore walls. The connate water phase within strongly oil-wet medium remained in the form of small individual trapped drops surrounded by thick continuous oil layers (saturation), which has been shown in Fig. 4b. These small individual trapped water drops are considered as pseudo connate water saturation in this article.

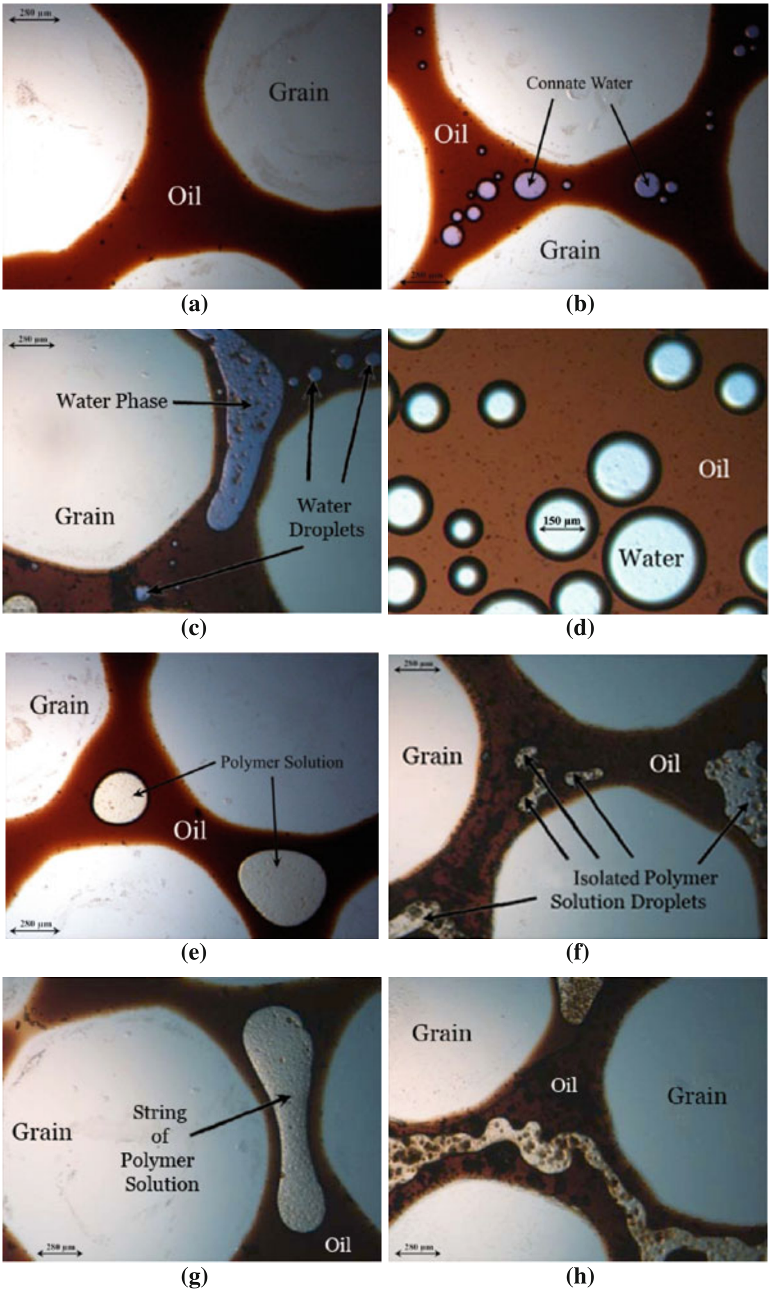

(a) (b) (c) (d) (e) (f) (g) (h)

Fig. 4 Microshots in strongly oil-wet medium captured under digital microscope. **a** Initial conditions: no connate water film; **b** Initial conditions: pseudo connate water; **c** Poor waterflooding performance; **d** Water–oil interaction during waterflooding; **e** Polymer solution trapping; **f** Isolated polymer solution droplets; **g** Discontinuous polymer solution string; **h** Continuous polymer solution string; **i** Polymer solution snap-off; **j** Partial sweep by polymer solution; **k** Distorted polymer solution; **l** Trapped emulsified residual oil; **m** Trapped oil saturation; **n** Piston-type displacement of oil; **o** Emulsified small trapped oil droplets; **p** Surface roughness of pore walls

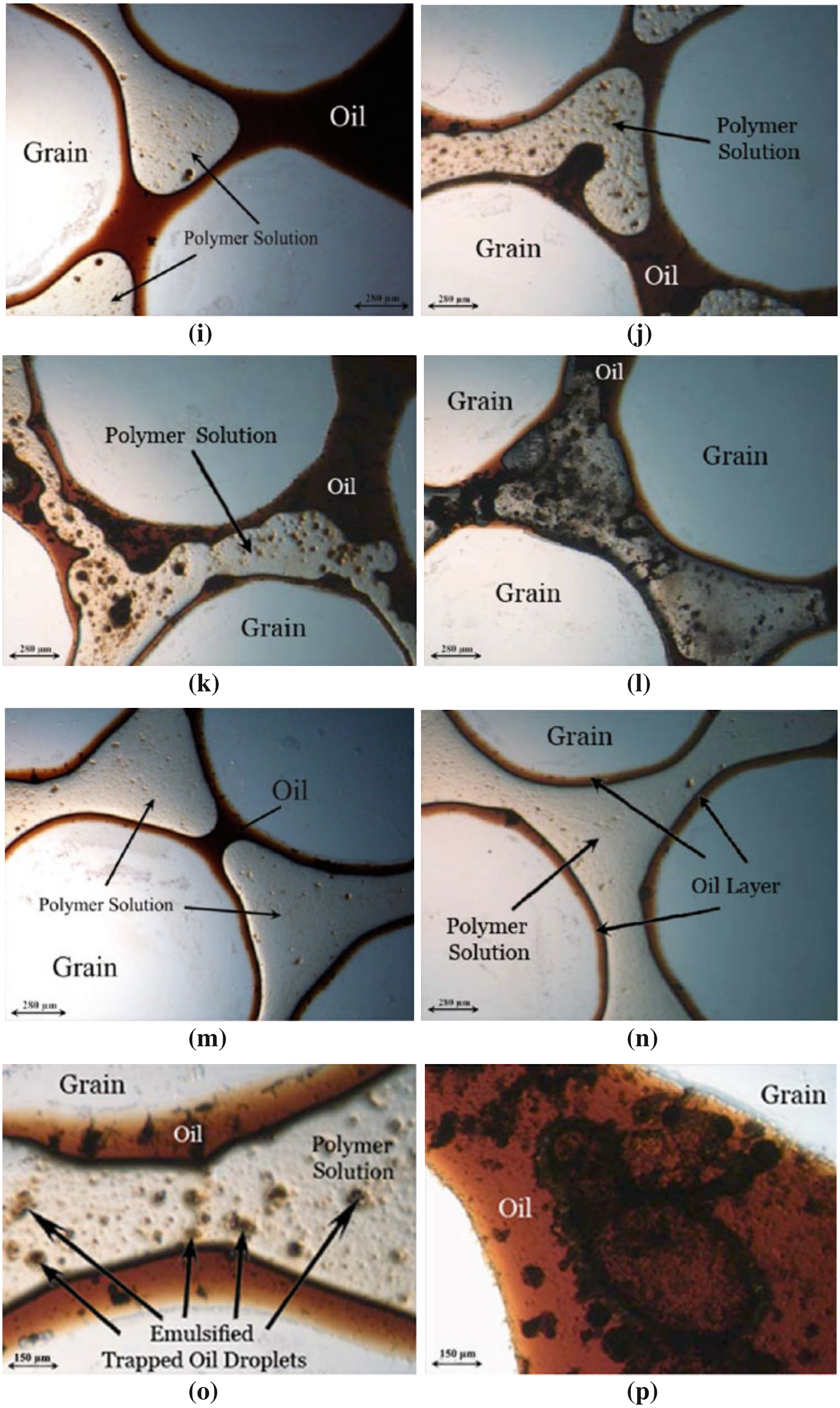

Fig. 4 continued

Figure 4c and d shows the poor performance of waterflooding in the oil-wet medium as the water phase flows in the middle of pore body and neck mainly in the form of partially discontinuous water phase (Fig. 4c) or small and large water phase droplets (Fig. 4d). This distribution of water phase during the waterflood in the oil-wet medium leaded to a very low microscopic displacement efficiency and thus poor macroscopic performance of waterflooding.

During polymer flooding in an oil-wet medium, continuous and discontinuous strings of polymer solution were observed within the pore neck and body (Fig. 4g and h). This was because of the nature of the pore walls. The polymer solution could not adhere onto the pore wall surface and preferred to flow in the middle of pore necks and bodies within oil-wet medium. On some occasions, polymer solution formed strings. These strings became either continuous and thin (Fig. 4h) or discontinuous and thicker (Fig. 4g). Polymer solution can be squeezed by capillary forces, while passing through a pore neck and forms a string. Since the interfacial tension between oil and polymer is less than oil and water, this string can be very thin but not discontinuous. In other words, under these conditions polymer solution snap-off is less likely to occur.

During the test, it was observed that trapping of polymer solution occurred frequently in the oil-wet medium (Fig. 4e). In this medium, the polymer solution (nonwetting phase) was trapped as isolated droplets while it was displacing oil (wetting phase). The isolated polymer solution droplets were held by strong capillary forces that could not be overcome by the relatively small viscous forces. However, the trapped polymer solution was mobilized when the capillary number (i.e., the ratio of viscous force to capillary force) became higher (Chatzis and Morrow 1984; van der Mark et al. 1997). The competition of viscous and capillary forces usually occurs over very short distances, most likely a few pore lengths. Moreover, the viscosity of the polymer solutions also plays an important role in the efficiency of microscopic displacement. The viscosity of polymer solution increases with increasing molecular weight, concentration of polymer, and degree of hydrolysis (Mungan et al. 1966; Martin and Sherwood 1975; Wang et al. 2001).

In an oil-wet medium, oil can be trapped in pore necks or totally bypassed due to the snap-off of the polymer solution (Roof 1970), which is shown in Fig. 4i and j. Under certain conditions depending on the wettability and pore structure, where pore neck is considerably smaller than pore body, an excess capillary pressure is built in the pore body as the polymer solution enters the pore neck because the radius of the pore body is greater than the radius of pore neck, causing snap-off (Blunt 1998; Lenormand et al. 1983; Roof 1970). Consequently, polymer solution loses its usual continuous configuration and appears to be in the form of either discontinuous polymer solution strings or isolated polymer solution droplets.

Figure 4k and l illustrates the partial sweep of an oil-wet section and trapping of polymer solution. It is seen that the polymer solution cannot sweep a strongly oil-wet medium completely. Figure 4m shows the similar results, where continuous flow of polymer solution fails to occur in some spots, particularly in pore necks. Nevertheless, the polymer solution occasionally could maintain its continuity within pore bodies and necks and displaced oil under the influence of displacement capillary pressure as shown in Fig. 4n. During this piston-like displacement of oil (Blunt 1998; Dixit et al. 1998; Lenormand et al. 1983), oil layers coated the oil-wet grain surfaces and the polymer solution flowed through the middle of pore bodies and necks and close to the pore walls. Polymer flooding was controlled by the piston-like displacement of oil and polymer solution snap-off in the strongly oil-wet medium.

In the oil-wet medium, discontinuity in polymer solution was observed to occur in different portions. In Fig. 4m, it can be seen that this discontinuity occurs within pore necks of the porous medium. Figure 4g and k presents two other forms of discontinuity in polymer solution. In these two microshots as shown, discontinuity in polymer solution occurred within both pore bodies and necks.

Formation of emulsions was observed during polymer flooding within an oil-wet medium. In contrast to microemulsions which are a stable system of water, oil, and surfactant, frequently in combination with a cosurfactant (Danielsson and Lindman 1981), emulsion requires high shear conditions (i.e., high viscous forces) to be formed. Although these emulsions were unstable, their formation contributed to the transport of oil (dispersed phase) within polymer solution (continues phase) until the associated oleic phase was produced simultaneously with the polymer solution at the production outlet. On these occasions, the interface of the polymer solution was observed to be distorted (Fig. 4k and l). In Fig. 4l, it is readily observed that emulsions were formed, but emulsified oil was not produced from the outlet as it was trapped within the oil-wet medium and form a part of residual oil saturation distributed throughout the medium. Also, it was observed that the polymer solution had a cloudy appearance because many interfaces scattered the light, which passed through the trapped emulsified oil within polymer solution. In other words, the translucent-to-dark color of the polymer solution was attributed to the emulsification and subsequent trapped of the oleic phase within the polymer solution (Fig. 4o). Existence of irregularities in pore bodies and necks and roughness of grain surfaces was one of the factors contributing to the distorted flow of polymer solution (Fig. 4k) and may also cause the formation of emulsions. The roughness of the grain surfaces may reduce the residual saturation of wetting phase (i.e., oil phase in oil-wet system and polymer solution in water-wet) to a very low value with the increase of the externally applied pressure (Dullien et al. 1989; Morrow 1970). Nonetheless, the surface roughness of the pores makes the oil phase bond more strongly within the oil-wet medium. Accordingly, a higher viscous force is needed to produce the same amount of oil from the porous medium compared to the smooth grain surfaces. However, in a water-wet porous medium, the roughness will bond the water to the grain surface and facilitate improving the microscopic sweep efficiency.

In a strongly water-wet porous medium, relatively thick connate water films were formed on the pore walls because water tends to spread on the grain surfaces (Fig. 5a) and wets the whole pore walls.

Waterflooding in a strongly water-wet medium can result in higher oil sweep efficiency in the porous medium as shown in Fig. 5b and c.

Figure 5d shows the middle state of polymer flooding where unswept oil within the micromodel remained due to the high capillary pressure of the unswept site. In the final state, some parts of the glass micromodel with residual oil saturation are presented in Fig. 5e–g. In this figure, polymer solution has displaced most of the oil. Moreover, in Fig. 5e, it can be seen that the discontinuity of polymer solution occurred within the pore necks in the strongly water-wet medium, while the discontinuity of polymer solution occurred in both pore bodies and pore necks in strongly oil-wet medium as discussed previously.

On some occasions, it was observed that the oil phase was bypassed by the polymer solution where the thick connate water film existed on the grain surfaces (Fig. 5f). When polymer solution was surrounded by the thick films of connate water, it tended to finger inside the pore neck and flow in the middle of pore neck and then bypass the oil phase (Fig. 5g). Nevertheless, in some other parts of the strongly water-wet medium, it was surprisingly observed that the oil phase was bypassed between the polymer solution and pore walls (Fig. 5d and e). This could result from the wettability alteration from strongly water-wet to moderate water-wet by asphaltene droplets.

The complete microscopic pore-to-pore sweep of oil phase existing within pore bodies and necks by polymer solution was mainly observed through the experiment conducted in

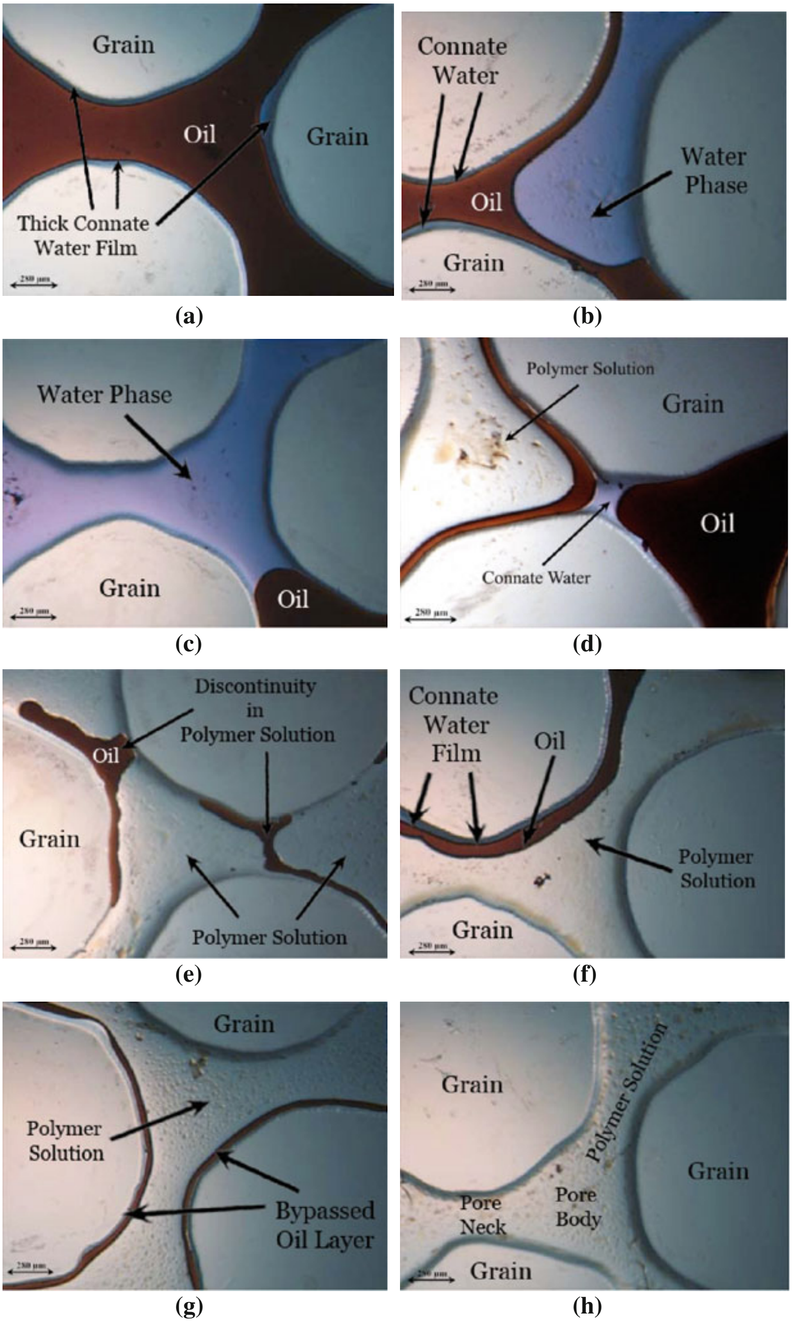

Fig. 5 Microshots in strongly water-wet medium captured under digital microscope; **a** Initial conditions: connate water film; **b** Intermediate efficiency of waterflood; **c** Efficient sweeping in waterflooding; **d** Unswept oil after polymer flooding; **e** Discontinuity in polymer solution; **f** Bypassed think layer of oil by polymer; **g** Partial sweeping by polymer solution; **h** Complete microscopic sweep by polymer

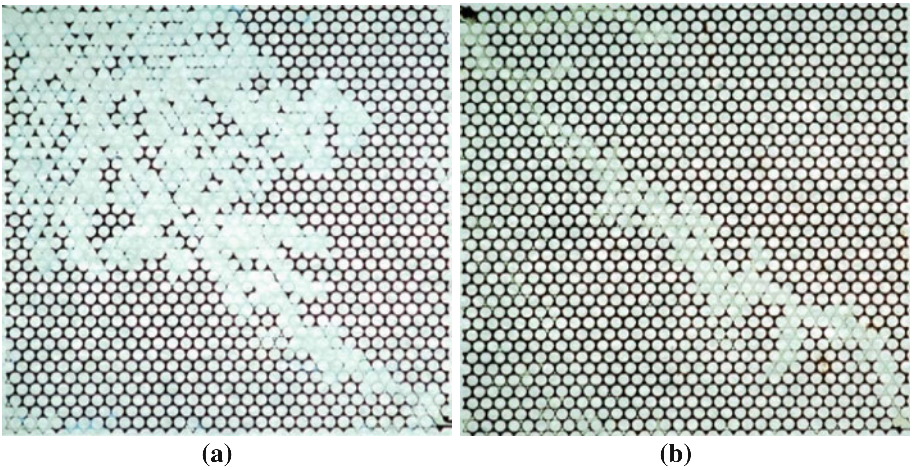

Fig. 6 Displacement front for waterflooding at breakthrough time in strongly **a** water-wet medium and **b** oil-wet medium

the strongly water-wet medium. This was one of the reasons for the efficient macroscopic performance of polymer flooding in the strongly water-wet medium. The polymer solution in the strongly water-wet medium generally tended to adhere to the pore walls, and thereby resulted in an almost 100% microscopic sweep efficiency within some portions of strongly water-wet medium (Fig. 5h). This did not often occur within strongly oil-wet medium.

Connate water can make viscous fingering pattern more irregular and reduce oil recovery through a low flowrate waterflood process (Thibodeau et al. 1997). However, it was observed that the thick layer of connate water assisted the polymer solution to displace the oil phase by reducing the resistance between the polymer solution and grain surfaces, which resulted in complete microscopic pore-to-pore sweep of oil phase. Nevertheless, the thick layer of connate water could mix with the polymer solution and degrade the quality of polymer.

3.2 Macroscopic Observations

The displacement fronts at breakthrough time during a waterflood in strongly water-wet and oil-wet media are shown in Fig. 6a and b, respectively. It can be seen from this figure that the displacement front in the water-wet medium is more uniform than in an oil-wet medium, which is consistent with what has been presented by Craig (1971). Essentially, wettability not only plays a major role in controlling the location, flow, and distribution of oil and water phases but also affects the relative permeability of a porous medium (Anderson 1987). More precisely, the water relative permeability is higher in an oil-wet medium than in the a water-wet medium, which accordingly leads to a higher mobility ratio in the oil-wet medium than that in the water-wet medium. As discussed earlier, the mobility ratio also can be optimized by adding polymer into the water so that the viscosity of the water phase increases.

The displacement front of polymer 1 ($\mathrm{MW_p} = 1.6 \times 10^6$ g/mol) as a function of polymer concentrations at breakthrough time in strongly water-wet and oil-wet media are shown in Fig. 7a–f, respectively. Figure 7a, c and e illustrates the displacement front for polymer flooding with the concentration of 100, 300, and 500 ppm, respectively (i.e., tests 2, 3, and 4, respectively). The apparent viscosity of the polymer solution increases with the polymer concentration, which accordingly results in a lower oil–polymer viscosity ratio and consequently a higher macroscopic sweep efficiency. Figure 7b, d, and f illustrates the displacement front of polymer flooding in a strongly oil-wet medium with concentrations of 100, 300, and 500 ppm, respectively (i.e., tests 13, 14, and 15, respectively). At a higher polymer concentration, the macroscopic sweep efficiency increases. However, the stability of the displacement front was hardly improved by increasing the polymer concentration, which is contrary to what was observed in the strongly water-wet medium. Moreover, the polymer solution fingered toward the outlet in the oil-wet medium due to the influence of porous medium wettability. In other words, polymer solution fingering occurs because of the adverse microscopic mechanisms which significantly influence the fluid displacement process in the oil-wet medium. In contrast, the favorable active microscopic mechanism in the water-wet medium resulted in a relatively uniform front and enhanced the macroscopic sweep efficiency.

Figure 8a–h shows the displacement front at breakthrough time for polymer 2 in the strongly water-wet and oil-wet media, respectively. Figure 8a, c, e, and g illustrates the displacement front in a strongly water-wet medium with the concentration of 100, 300, 500, and 700 ppm, respectively (i.e., tests 5, 6, 7, and 8, respectively). In Fig. 8b, d, f, and h, the polymer concentration (polymer 2) also increases from 100 to 700 ppm and the trend of the displacement front at breakthrough time in a strongly oil-wet medium is shown. In general, for polymer 2, changes on the pattern of the displacement front at breakthrough time in strongly oil-wet and water-wet media are the same as for polymer 1.

Figure 9 shows the displacement front at breakthrough time for polymer 3 in strongly water-wet and oil-wet media. Figure 9a, c, and e illustrates the displacement front in strongly water-wet medium with the concentration of 100, 300, and 500 ppm, respectively (i.e., tests 9, 10, and 11, respectively). In Fig. 9b, d, and f, the polymer concentration (polymer 3) increases from 100 to 500 ppm and the trend of the pattern of the displacement front at breakthrough time in strongly oil-wet medium are shown. Again, for polymer 3, the trends of the pattern of the displacement front at breakthrough time in strongly water-wet and oil-wet media similar to those results obtained using polymers 1 and 2.

To sum up, the pattern of the displacement front at breakthrough time in the strongly water-wet and oil-wet medium show similar trends for polymers 1, 2, and 3 with the increase of polymer concentration (i.e., decrease of oil–polymer viscosity ratio). In the water-wet medium, the polymer solution spread uniformly in the micromodel and formed a wide stable front. However, when polymer solution moved about half way through the micromodel, it started to finger towards the outlet, which has a low pressure. In the oil-wet medium, polymer solution fingering started from the injection point and a stable polymer solution front did not occur, which is due to the influence of porous media wettability on forming the thin and continuous stream of polymer solution.

3.3 Quantitative Evaluations and Implications

3.3.1 Waterflooding Performance

The results of waterflooding experiments in the glass micromodel with strongly water-wet and oil-wet conditions are listed in Table 4. These show that the oil recovery from waterflooding at strongly water-wet conditions was much higher than that when conditions were strongly oil-wet, which is attributed to the different relative permeabilities in the oil-wet and water-wet porous media. According to the data in Table 4, it can be seen that the breakthrough for water-wet medium happens later than an oil-wet medium. From the microscopic point of view,

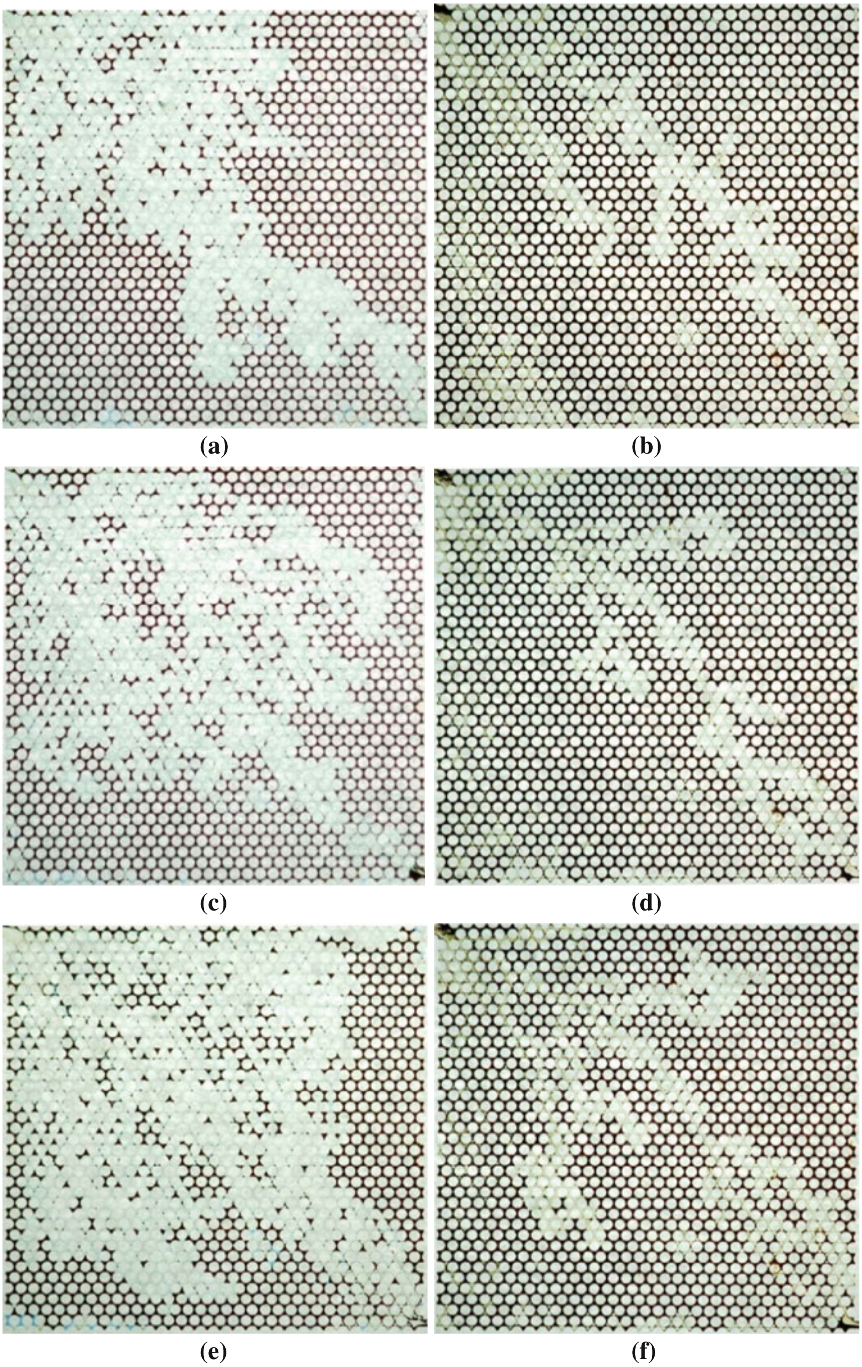

(a) (b) (c) (d) (e) (f)

Fig. 7 Displacement front for polymer 1 ($MW_p = 1.6 \times 10^6$ g/mol) at breakthrough time in oil-wet and water-wet media. **a** 100 ppm, water-wet; **b** 100 ppm, oil-wet; **c** 300 ppm, water-wet; **d** 300 ppm, oil-wet; **e** 500 ppm, water-wet; **f** 500 ppm, oil-wet

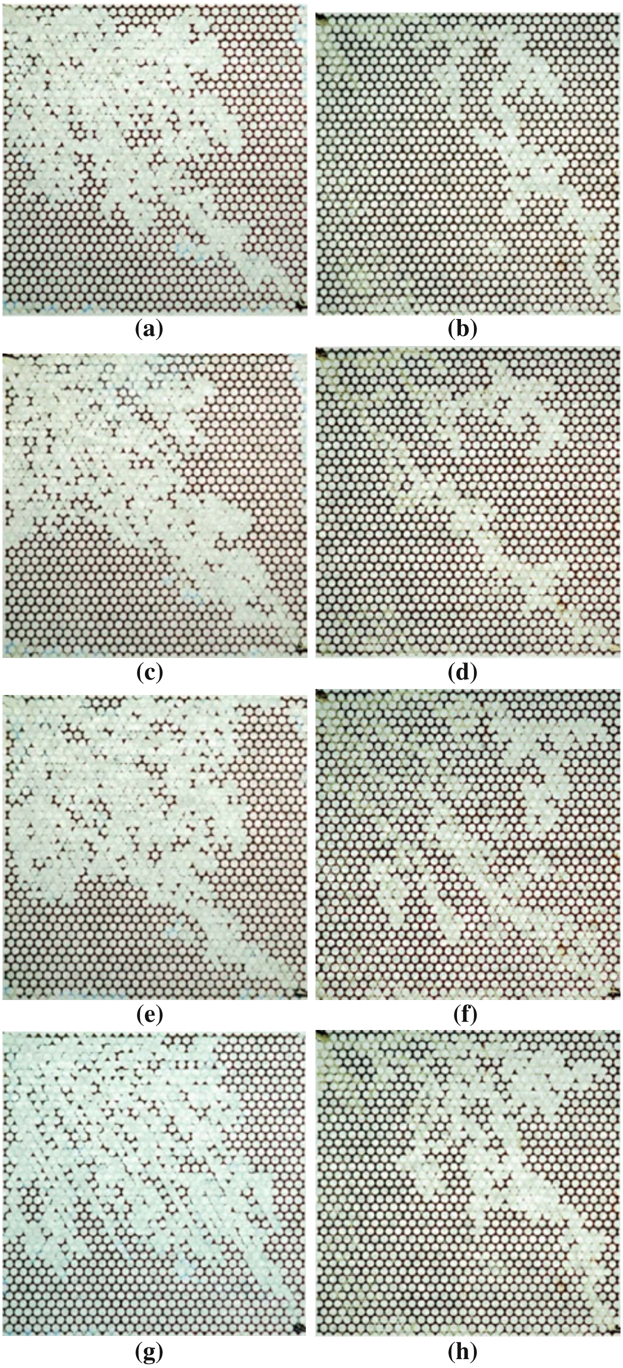
(a) (b) (c) (d) (e) (f) (g) (h)

Fig. 8 Displacement front for polymer 2 ($MW_p = 8 \times 10^6$ g/mol) at breakthrough time in oil-wet and water-wet media. **a** 100 ppm, water-wet; **b** 100 ppm, oil-wet; **c** 300 ppm, water-wet; **d** 300 ppm, oil-wet; **e** 500 ppm, water-wet; **f** 500 ppm, oil-wet; **g** 700 ppm, water-wet; **h** 700 ppm, oil-wet

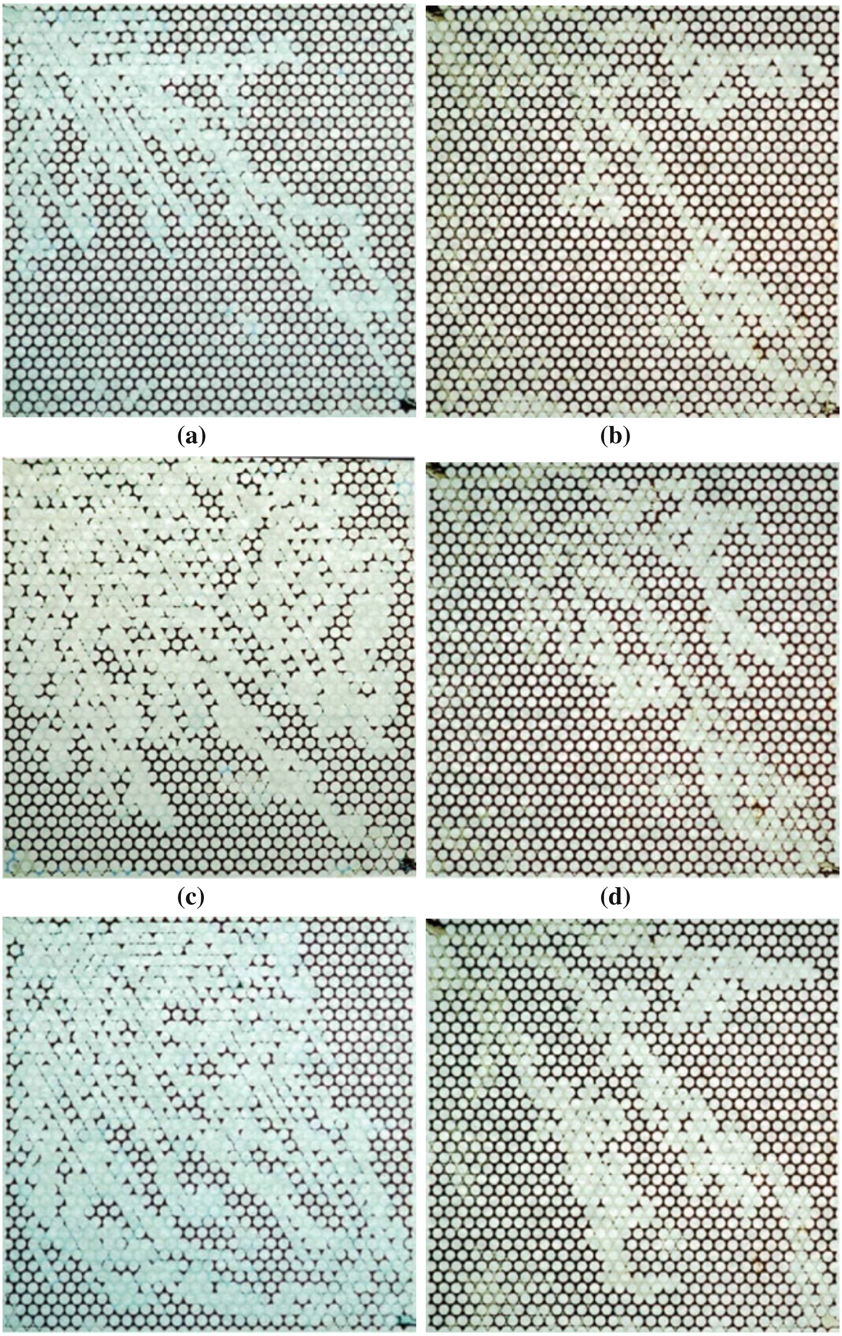

(a) (b) (c) (d) (e) (f)

Fig. 9 Displacement front for polymer 3 ($MW_p = 12 \times 10^6$ g/mol) at breakthrough time in oil-wet and water-wet media. **a** 100 ppm, water-wet; **b** 100 ppm, oil-wet; **c** 300 ppm, water-wet; **d** 300 ppm, oil-wet; **e** 500 ppm, water-wet; **f** 500 ppm, oil-wet

Table 4 Breakthrough and ultimate oil recovery: waterflooding

Test no.	Wetting nature	Viscosity ratio	BT (min)	R_B(%)	$R_{1.5\,IPV}$(%)
1	Water-wet	65.8	33	40.0	48.6
12	Oil-wet	65.8	12	14.9	18.2

Table 5 Breakthrough and ultimate oil recovery: polymer flooding

Test no.	Wetting nature	MW_p ($\times 10^6$ g/mol)	C_p(ppm)	Viscosity ratio	BT (min)	R_B(%)	$R_{1.5\,IPV}$(%)
3	Water-wet	1.6	300	14.5	38	49.0	57.9
5	Water-wet	8	100	33.4	31	40.5	49.6
6	Water-wet	8	300	16.1	36	45.1	52.8
7	Water-wet	8	500	9.8	37	47.8	55.5
8	Water-wet	8	700	6.7	39	51.0	56.8
10	Water-wet	12	300	12.1	41	53.7	60.1
14	Oil-wet	1.6	300	14.5	19	24.3	28.9
16	Oil-wet	8	100	33.4	14	17.7	22.0
17	Oil-wet	8	300	16.1	19	24.0	28.7
18	Oil-wet	8	500	9.8	21	26.8	33.6
19	Oil-wet	8	700	6.7	23	30.5	37.9
21	Oil-wet	12	300	12.1	19	25.1	30.8

this was because brine has much less tendency to stick to the pore body and throat walls in an oil-wet medium compared to in a water-wet medium and thus it can channel to the production side more rapidly. Recovery factors at breakthrough (BT) and 1.5 pore volumes (PV) injected in a water-wet medium were generally higher than those in the oil-wet medium, which is in agreement with Anderson (1987). Moreover, recovery factors in the oil-wet medium after breakthrough changed slightly (from 14.9 to 18.2% OOIP), while they changed more (from 40.0 to 48.6% OOIP) in the strongly water-wet medium after breakthrough. The relatively great increase in oil recovery after water breakthrough in the strongly water-wet medium demonstrates the effect of wettability on the performance of waterflooding.

3.3.2 Polymer Flooding Performance

Since the viscosity of polymer solution is dramatically affected by the polymer molecular weight, concentration, and the degree of hydrolysis, it is expected that these will significantly affect the performance of polymer flooding and oil recovery value. Experimental results for polymer flooding with different polymer molecular weights (i.e., 1.6, 8, 12 $\times 10^6$ g/mol) and concentrations (i.e., 100, 300, 500, and 700 ppm) are given in Table 5. It can be seen from the table that the recovery factors at different polymer molecular weights and concentrations are much higher in a water-wet medium than those in an oil-wet medium. In addition, recovery factors in a oil-wet medium after breakthrough change less significantly in comparison to those in the water-wet medium. It shows that the lower oil–polymer viscosity ratios can result in higher recovery factors at both oil-wet and water-wet porous mediums. This is because a lower viscosity ratio leads to a lower mobility ratio.

In addition, the effects of polymer concentration on oil recovery at different wettability conditions are different (compare test 6 to 17 and 7 to 18). As shown in Table 5, recovery factor for a polymer with a higher degree of hydrolysis (25–30%) and lower value of molecular weight (1.6×10^6) is higher than the corresponding recovery values for a polymer with higher molecular weight (8×10^6) and lower degree of hydrolysis (20–25%) (compare test 3 to 6). As mentioned above, a higher degree of hydrolysis means a greater apparent viscosity and lower oil–polymer viscosity ratio. On the other hand, the apparent viscosity increases with the molecular weight of polymer. This illustrates that, under these experimental conditions, the degree of hydrolysis has a stronger influence on the apparent viscosity of polymer solution than the molecular weight. Moreover, in the oil-wet medium with the same condition existing in water-wet medium, the effect of polymer hydrolysis on the recovery factor is less significant compared to that in the water-wet medium (see tests 14 and 17). This behavior is due to the adverse microscopic displacement mechanisms within the oil-wet medium.

In conclusion, the experimental results show that a general increasing trend exists for the breakthrough time and ultimate recovery factors (i.e., recovery at 1.5 injected pore volume) as the polymer concentration of the injected polymer solution increases for both wettability conditions. Furthermore, polymer flooding in the strongly water-wet medium shows higher recovery factors in comparison to the strongly oil-wet medium at different polymer concentrations. Based on these results, trends of ultimate recovery factors at 1.5 injected pore volumes in polymer flooding at relatively low (i.e., 100 ppm) and intermediate (i.e., 300 and 500 ppm) polymer concentrations for water-wet (tests 5, 6, and 7) and oil-wet media (16, 17, and 18) increase with the polymer concentration. However, the increase of ultimate recovery values with the polymer concentration in the oil-wet medium at relatively low and intermediate polymer concentrations is relatively sharper than that in the water-wet medium. This is because of the wettability effects on the relative permeabilities and consequently the mobility ratio.

4 Summary and Conclusions

In this study, two waterflood and twenty polymer flood experiments were conducted in a homogeneous two-dimensional glass micromodel under strongly oil-wet and water-wet conditions to investigate the effects of wettability on the microscopic and macroscopic efficiency of polymer oil recovery. In order to study the effects of viscosity ratio, three polyacrylamides with different molecular-weight and degree of hydrolysis were used to prepare polymer solutions with different concentrations and conduct the later polymer flood experiments. Following conclusions were drawn based on the results of this study:

(1) In the strongly water-wet medium, thick connate water films were observed on the pore walls. Complete microscopic pore-to-pore sweep of the oil phase was frequent and discontinuity of polymer solution occurred mainly within the pore necks. The favorable microscopic displacement mechanism resulted in a relatively uniform front and enhanced the macroscopic sweep efficiency.

(2) In the strongly oil-wet medium, no thick connate water film was observed on grain surfaces. Instead, a trapped water phase within the oil phase was observed and considered as a pseudo connate water saturation. Complete trapping of polymer solution was observed to occur but polymer solution rarely if ever completely swept the oil. Moreover, the discontinuity in polymer solution occurred within both pore bodies and

necks. Emulsion formation contributed to the transport of oil phase within the polymer solution. Also, the competition between piston-like displacement of oil and polymer solution snap-off as well as the competition between capillary and viscous forces had a significant influence on the microscopic displacement, stability of front, and oil recovery.

(3) Generally, the pattern of flow, stability of polymer solution front, and ultimate oil recovery were controlled by the mobility ratio, which was considerably influenced by the wettability of the porous medium and the apparent viscosity of the polymer solution. The apparent viscosity of the polymer solution increased with the polymer molecular weight, degree of hydrolysis, and concentration, which means a lower oil–polymer viscosity ratio or mobility ratio. On the other hand, different wettabilities of the porous medium can result in different relative permeabilities and different mobility ratios.

(4) Oil recovery at the breakthrough and the end of the experiment in the water-wet medium was much higher than that in the oil-wet medium. In addition, the recovery factor in the oil-wet medium after breakthrough changes less significantly in comparison to that in the water-wet medium. For both oil-wet and water-wet media, recovery factors were higher at lower viscosity ratios.

Acknowledgments This work was carried out with financial support from the National Iranian Oil Company (NIOC). The authors thank Petroleum University of Technology Research Center, Iran Polymer and Petrochemical Institute (Department of Process Modeling and Control), and Research Institute of Petroleum Industry (Polymer Science and Technology Research Division) for providing technical support and the laboratory facilities. The authors also thank reviewers for useful comments. Finally, the first author thanks Benyamin Yadali Jamaloei at the University of Calgary for technical discussions.

References

Anderson, W.G.: Wettability literature survey. Part 1: Rock-oil-brine interactions and effects of core handing on wettability. SPE 13932. J. Pet. Technol. **38**(10), 1125–1143 (1986)

Anderson, W.G.: Wettability literature survey. Part 6: The effect of wettability on water flooding. SPE 16471. J. Pet. Technol. **39**(12), 1605–1622 (1987)

Blunt, M.J.: Physically-based network modeling of multiphase flow in intermediate-wet porous media. J. Pet. Sci. Eng. **20**(3–4), 117–125 (1998)

Broseta, D., Medjahed, F., Lecourtier, J., Robin, M.: Polymer adsorption/retention in porous media: effects of core wettability and residual oil. SPE 24149. SPE Adv. Technol. Ser. **3**(1), 103–112 (1995)

Buckley, J.S., Morrow, N.R.: Characterization of crude oil wetting behavior by adhesion tests. In: SPE 20263. SPE/DOE Seventh Symposium on Enhanced Oil Recovery, Tulsa, USA, 21–25 April (1990)

Chang, H.L.: Polymer flooding technology—yesterday, today, and tomorrow. SPE 7043. J. Pet. Technol. **30**(8), 1113–1128 (1978)

Chatzis, I., Morrow, N.R.: Correlation of capillary number relationships for sandstone. SPE 10114. SPE J. **24**(5), 555–562 (1984)

Craig, F.F.: The Reservoir Engineering Aspects of Waterflooding. Monograph Series. SPE, Richardson (1971)

Cuiec, L.E., Anderson, B.: Evaluation of reservoir wettability and its effects on oil recovery. In: Morroe, N.R. (ed) Interfacial Phenomena in Oil Recovery, pp. 319–375. Marcell Dekker, New York (1990)

Danielsson, I., Lindman, B.: The definition of microemulsion. Colloids Surf. **3**(4), 391–392 (1981)

Dawe, R.A., Zhang, Y.: Mechanistic study of the selective action of oil and water penetrating into a gel emplaced in a porous medium. J. Pet. Sci. Eng. **12**(2), 113–125 (1994)

Dixit, A.B., McDougall, S.R., Sorbie, K.S.: A pore-level investigation of relative permeability hysteresis in water-wet systems. SPE 37233. SPE J. **3**(2), 115–123 (1998)

Donaldson, E.C., Chilingarian, G.V., Yen, T.F.: Enhanced Oil Recovery, II: Processes and Operations. Elsevier, Amsterdam (1989)

Dong, H., Hong, Y., Rui, W., Fan, D.: The effect of wettability on oil recovery of alkaline/surfactant/polymer flooding. In: SPE 102564. SPE Annual Technical Conference and Exhibition, San Antonio, Texas, USA, 24–27 September (2006)

Dubey, S.T., Waxman, M.H.: Asphaltene adsorption and desorption from mineral surfaces. SPE 18462. SPE Reserv. Eng. **6**(3), 389–395 (1991)

Dullien, F.A.L, Zarcone, C., Macdonald, I.F., Collins, A., Bochard, R.D.E: The effects of surface roughness on the capillary pressure curves and the heights of capillary rise in glass bead packs. J. Colloid Interface Sci. **127**(2), 362–372 (1989)

Elmkies, Ph., Bertin, H., Lasseux, D., Murray, M., Zaitoun, A.: Further investigations on two-phase flow property modification by polymers: wettability effects. In: SPE 64986. SPE International Symposium on Oilfield Chemistry, Houston, Texas, USA, 13–16 February (2001)

Emami Meybodi, H., Kharrat, R., Ghazanfari, M.H.: Effect of heterogeneity of layered reservoirs on polymer flooding: an experimental approach using five-spot glass micromodel. In: SPE 113820. SPE Europec/EAGE Annual Conference and Exhibition, Rome, Italy, 9–12 June (2008)

Gogarty, W.B.: Mobility control with polymer solutions. SPE 1566. SPE J. **7**(2), 161–173 (1967)

Green, D.W., Willhite, G.P.: Enhanced Oil Recovery. Textbook Series vol. 6, 2nd edn. Society of Petroleum Engineers, Richardson (2003)

Haghighi, M., Yortsos, Y.C.: Visualization of steam injection in fractured systems using micromodels. In: SPE 37520. SPE International Thermal Operation and Heavy Oil Symposium, Bakersfield, California, USA, 10–12 February (1997)

Jadhunandan, P.P., Morrow, N.R.: Effect of wettability on water flood recovery for crude-oil/brine/rock system. SPE 22597. SPE Reserv. Eng. **10**(1), 40–46 (1995)

Jewett, R.L., Schurz, G.F.: Polymer flooding—a current appraisal. SPE 2545. J. Pet. Technol. **22**(6), 675–684 (1970)

Jia, D., Buckley, J.S., Morrow, N.R.: Control of core wettability with crude oil. In: SPE 21041. SPE International Symposium on Oilfield Chemistry, Anaheim, California, USA, 18–21 February (1991)

Larsen, J.K., Bech, N., Winter, A.: Three-phase immiscible wag injection: micromodel experiments and network models. In: SPE 59324. SPE/DOE Improved Oil Recovery Symposium held in Tulsa, Oklahoma, USA, 3–5 April (2000)

Lenormand, R., Zarcone, C., Sarr, A.: Mechanisms of the displacement of one fluid by another in a network of capillary ducts. J. Fluid Mech. **135**, 337–353 (1983)

Martin, F.D., Sherwood, N.S.: The effect of hydrolysis of polyacrylamide on solution viscosity, polymer retention and flow resistance properties. In: SPE 5339. SPE-AIME Rocky Mountain Regional Meeting, Denver, Colorado, USA, 7–9 April (1975)

Morrow, N.R.: Physics and thermodynamics of capillary action in porous media. Ind. Eng. Chem. **62**(6), 32–56 (1970)

Morrow, N.R.: Wettability and its effect on oil recovery. SPE 21621. J. Pet. Technol. **42**(12), 1476–1484 (1990)

Mungan, N.: Rheology and adsorption of aqueous polymer solutions. J. Can. Pet. Technol. **8**(2), 45–50 (1969)

Mungan, N., Smith, F.W., Thompson, J.L.: Some aspects of polymer floods. SPE1628. J. Pet. Technol. **18**(9), 1143–1150 (1966)

Nasr-El-Din, H.A., Taylor, K.C.: Interfacial behaviour of crude oil/alkali systems in the presence of partially hydrolysed polyacrylamide. Colloids Surf. A **75**, 169–183 (1993)

Needham, R.B., Doe, P.H.: Polymer flooding review. SPE 17140. J. Pet. Technol. **39**(12), 1503–1507 (1987)

Nilsson, S., Lohne, A., Veggel, K.: Effect of polymer on surfactant floodings of oil reservoirs. Colloids Surf. A **127**, 241–247 (1997)

Pye, D.J.: Improved secondary recovery by control of water mobility. SPE 845. J. Pet. Technol. **16**(8), 911–916 (1964)

Romero-Zerón, L.B.: The role of porous media wettability on foamed gel propagation and fluid diverting performance. Ph.D. Dissertation, University of Calgary, Calgary, Canada, October (2004)

Romero-Zerón, L.B., Ongsurakula, S., Lib, L., Balcombc, B.: Visualization of the effect of porous media wettability on polymer flooding performance through unconsolidated porous media using magnetic resonance imaging. Pet. Sci. Technol. **28**(1), 52–67 (2010)

Roof, J.G.: Snap-off of Oil droplets in water-wet pores. SPE J. **10**(1), 85–90 (1970)

Sandiford, B.B.: Laboratory and field studies of water floods using polymer solutions to increase oil recoveries. SPE 844. J. Pet. Technol. **16**(8), 917–922 (1964)

Smith, F.W.: The behavior of partially hydrolyzed polyacrylamide solutions in porous media. SPE 2422. J. Pet. Technol. **22**(2), 148–156 (1970)

Sparlin, D.: An evaluation of polyacrylamides for reducing water production. SPE 5610. J. Pet. Eng. **28**(8), 906–914 (1975)

Szabo, M.T.: Some aspects of polymer retention in porous media using C14-tagged hydrolyzed poly-acrylamide. SPE 4668. SPE J. **15**(4), 323–337 (1975)

Taugbol, K., Ly, T.V., Austad, T.: Chemical flooding of oil reservoirs 3. Dissociative surfactant-polymer interaction with a positive effect on oil recovery. Colloids Surf. A **103**, 83–90 (1995)

Thibodeau, L., Guo, T., Neale, G.H.: Effects of connate water on immiscible displacement processes in porous media. Powder Technol. **93**(3), 209–217 (1997)

Treiber, K.E., Archer, D.L., Owen, W.W.: A laboratory evaluation of the wettability of fifty oil producing reservoirs. SPE 3526. SPE J. **12**(6), 531–540 (1972)

Uren, L.C., Fahmy, E.H.: Factors influencing the recovery of petroleum from unconsolidated sands by waterflooding. AIME J. **77**, 318–335 (1927)

van der Mark, S.C., Matsuura, T., Glas, J.: Viscous and capillary pressures during drainage: network simulations and experiments. Phys. Rev. E **56**(5), 5675–5687 (1997)

Waldraw, N.C.: The effect of pore structure on displacement efficiency in reservoir rocks and in glass micromodels. In: SPE 8840. SPE/DOE Symposium on Enhanced Oil Recovery, Tulsa, Oklahoma, USA, 20–23 April (1980)

White, J.L., Phillips, H.M., Goddard, J.E., Baker, B.D.: Use of polymers to control water production in oil wells. SPE 3672. J. Pet. Technol. **25**(2), 143–150 (1973)

Wang, D.M., Xia, H.F., Liu, Z.C., Yang, Q.Y.: Study of the Mechanism of polymer solution with visco-elastic behavior increasing microscopic oil displacement efficiency and the forming of steady "oil thread" flow channels. In: SPE 68723. SPE Asia Pacific Oil and Gas Conference and Exhibition, Jakarta, Indonesia, 17–19 April (2001)

Yadali Jamaloei, B., Kharrat, R.: Fundamental study of pore morphology effect in low tension polymer flooding or polymer-assisted dilute surfactant flooding. Transp. Porous Med. **76**(2), 199–218 (2009)

Yadali Jamaloei, B., Kharrat, R.: Analysis of microscopic displacement mechanisms of dilute surfactant flooding in oil-wet and water-wet porous media. Transp. Porous Med. **81**(1), 1–19 (2010)